Canadian Mineralogist
Vol. 24, pp. 435-447 (1986)

HYDRONIUM ION IN THE ALUNITE – JAROSITE GROUP

JOHN A. RIPMEESTER AND CHRISTOPHER I. RATCLIFFE
Division of Chemistry, National Research Council of Canada, Ottawa, Ontario K1A 0R9

JOHN E. DUTRIZAC AND JOHN L. JAMBOR
CANMET, Energy, Mines and Resources Canada, 555 Booth Street, Ottawa, Ontario K1A 0G1

ABSTRACT

Deuterated hydronium alunite and various members of the hydronium–potassium-alunite solid-solution series were synthesized, and characterized chemically and structurally. The ^1H nuclear magnetic resonance (NMR) technique with magic-angle spinning was used to confirm the existence of hydronium ion in these compounds. The ^2H NMR lineshapes as a function of temperature are less conclusive, but show motional narrowing of the D_3O^+ and D_2O lineshapes between 77 and 160 K. A qualitative correlation between the NMR spectrum and the expected amount of hydronium ion in a member of the hydronium–potassium-alunite solid-solution series strongly suggests that observed alkali deficiencies are due to the charge-compensating substitution of hydronium ion for the alkali. The presence of "excess water" in the alunite, confirmed by NMR, may indicate that the hydronium ion is itself partly hydrated. By extension, the conclusions obtained for alunite most certainly also apply to jarosite.

Keywords: nuclear magnetic resonance, magic-angle spinning, deuterated hydronium alunite, hydronium–potassium-alunite, hydronium jarosite, solid solution, hydronium ion.

SOMMAIRE

L'alunite à hydronium deutérisé de même que certains membres de la solution solide d'alunite à hydronium–potassium ont été synthétisés et caractérisés au double point de vue chimique et structurel. On a employé la technique de résonance magnétique nucléaire (RMN) de ^1H avec spin à l'angle magique, pour confirmer l'existence de l'ion hydronium dans ces composés. Les profils de bandes RMN ^2H en fonction de la température, quoique moins concluants, ont tout de même démontré un rétrécissement de mouvement des profils de bandes D_3O^+ et D_2O entre 77 et 160 K. La corrélation qualitative entre le spectre RMN et la quantité prévue d'ion hydronium dans un membre de la solution solide d'alunite hydronium–potassium indiquerait fortement que les déficiences en alcalin observées sont dûes à une substitution d'ion hydronium à l'alcalin, avec compensation de charge. La présence d'eau en excès dans l'alunite, confirmée par RMN, pourrait signifier que l'ion hydronium est lui-même partiellement hydraté. Par analogie, on peut dire que les conclusions obtenues pour l'alunite sont valides aussi pour la jarosite.

Mots-clés: résonance magnétique nucléaire, spin à l'angle magique, alunite à hydronium deutérisé, alunite à potassium-hydronium, jarosite à hydronium, solution solide, ion hydronium.

INTRODUCTION

Minerals of the alunite–jarosite group have the general formula $MA_3(SO_4)_2(OH)_6$, where M is H_3O^+, Na^+, K^+, Rb^+, Ag^+, Tl^+, NH_4^+, $\frac{1}{2}Pb^{2+}$ or $\frac{1}{2}Hg^{2+}$ and A is Al^{3+} (alunite group) or Fe^{3+} (jarosite group). Members of the group are isostructural, with hexagonal space-group $R\bar{3}m$, although structural anomalies such as doubled cells are occasionally noted (Wang *et al.* 1965, Menchetti & Sabelli 1976, Goreaud & Raveau 1980, Szymański 1985). Within the group, complete solid-solution exists for various M-site ions (Shishkin 1951, Dutrizac 1983); furthermore, complete solid-solution also has been demonstrated between some corresponding alunite and jarosite minerals (Brophy *et al.* 1962, Härtig *et al.* 1984), and likely exists for all alunite–jarosite species. Members of the alunite–jarosite group are relatively widespread in nature, and are occasionally of economic importance. Alunite is known to occur in extensive deposits that have been examined as alternative sources of alumina (Bengtson 1979). Jarosite is generally a useful indicator of sulfide mineralization and is occasionally sufficiently rich in Pb and Ag to constitute an ore of these metals (Schempp 1923). An unusual gallium-bearing jarosite is about to be exploited for its gallium values (Dutrizac *et al.* 1986). Recently, jarosite has assumed an important role in the metallurgical industry because precipitation of jarosite provides a ready avenue for the elimination of alkalis, iron and sulfate from hydrometallurgical processing solutions. Advantages cited for the jarosite precipitation route include the excellent settling and filtration properties of the precipitates, and low losses of sought-after divalent base-metals such as Zn^{2+}, Cu^{2+} and Ni^{2+} (Dutrizac 1979, 1982).

Many studies have been carried out to determine the interrelationships between precipitation conditions and the compositions of both alkali jarosite (Dutrizac 1983) and lead–silver jarosite (Dutrizac & Jambor 1985). When coupled with earlier investigations on the phase relationships among the various

members of the jarosite group, such studies have shown that jarosite-type compounds commonly deviate from the idealized chemical composition $M Fe_3(SO_4)_2(OH)_6$. There is generally a significant deficiency in alkali (*M*-site ion) and a modest deficiency in iron relative to $2(SO_4)$. Comprehensive studies of natural jarosite by Kubisz (1960, 1962, 1964) likewise indicated significant alkali and modest iron deficiencies. Similar phenomena also have been reported for the alunite minerals (Parker 1962, Wilkins *et al.* 1974), but the documentation is not as extensive as for jarosite. The deficiencies in both subgroups have been related to "excess" structural water, and it is generally assumed that the alkali (*M*-site) deficiencies are charge-compensated by the substitution of hydronium* ion for the various alkalis. That is, a more appropriate idealized formula for the alkali jarosite is $(M_{1-x}(H_3O)_x)_{1.00}Fe_3(SO_4)_2(OH)_6$. The value of x is in the range 0.1–0.3 for many samples of natural and synthetic jarosite.

Although end-member hydronium jarosite is readily synthesized (Posnjak & Merwin 1922), it is a relatively rare species in nature. Kubisz (1960), however, identified five samples of jarosite in which hydronium is the dominant *M*-site ion (Table 1). The data in Table 1 illustrate only the hydronium–alkali relationship, and ignore the commonly observed deficiencies in Fe^{3+} and the consequential conversion of OH^- to H_2O to maintain charge neutrality. Later, Kubisz (1961) elaborated on the formation of hydronium jarosite and stressed that this mineral forms only from alkali-deficient solutions, such as those originating from the rapid weathering of pyrite-bearing coal seams. The rarity of natural hydronium jarosite is clearly related to the ubiquitous presence of alkalis in groundwaters, and to the greater thermodynamic stability of the alkali jarosites, especially potassium jarosite.

Although the existence of end-member hydronium jarosite and hydronium-substituted alkali jarosite is accepted by the mineralogical community, proof of the existence of the ion species $(H_3O)^+$ is both tenuous and indirect. That is, the structure of "hydronium jarosite" can be conceived in several different ways, particularly if intermediate rather than the following end-member compositions are visualized:

$(H_3O^+)Fe_3(SO_4)_2(OH)_6$
M site occupied by hydronium ion

*Hydronium and oxonium are synonymous terms for H_3O^+. Oxonium is the preferred chemical term, but the mineralogical community favors hydronium, and the mineral name for $(H_3O)Fe_3(SO_4)_2(OH)_6$ is hydronium jarosite. The term *hydronium* has been used in this paper despite the fact that it is somewhat outdated in chemical terminology.

TABLE 1. LOCALITIES AND FORMULAS OF FIVE SAMPLES OF NATURAL HYDRONIUM JAROSITE*

Locality	Chemical Formula**
Thorez mine, Walbrzych, Poland	$(H_3O)_{0.88}Na_{0.07}K_{0.05}Fe_3(SO_4)_2(OH)_6$
Staszic mine, Holy Cross Mountain, Poland	$(H_3O)_{0.79}Na_{0.11}K_{0.10}Fe_3(SO_4)_2(OH)_6$
Malka mine, Caucasus, USSR	$(H_3O)_{0.76}K_{0.13}Na_{0.11}Fe_3(SO_4)_2(OH)_6$
Orzel Bialy mine, Upper Silesia, Poland	$(H_3O)_{0.56}(K,Na)_{0.39}Pb_{0.05}Fe_3(SO_4)_2(OH)_6$
Rudawka, Rymanowska, Carpathians, Poland	$(H_3O)_{0.50}K_{0.41}Na_{0.09}Fe_3(SO_4)_2(OH)_6$

* Data from Kubisz (1960)

**Only hydronium/alkali relationships are considered, and the Fe, SO_4 and OH contents are inferred to correspond to the idealized formula.

$(H_2O)Fe_3(SO_4)_2(OH)_5(H_2O)$
M site occupied by water

$Fe_3(SO_4)_2(OH)_5(H_2O)$
M site vacant

Chemical analysis of many natural and synthetic samples of jarosite (Kubisz 1964, Dutrizac & Kaiman 1976) shows significantly more water than suggested by the third option. Also, Johansson (1963) determined the crystal structure of synthetic $(H_3O)Ga_3(SO_4)_2(OH)_6$, which is isostructural with jarosite, and showed that the *M* site is occupied by an oxygen-bearing species, possibly H_3O^+ or H_2O. Hence, the *M* site seems to be occupied, most likely by either H_3O^+ or H_2O, but the choice between these alternatives is not obvious. The presence of H_3O^+ in close structural proximity to OH^- is intuitively unsatisfactory, and a reaction of the type

$$H_3O^+ + OH^- \rightarrow 2H_2O$$

might be expected, at least in part. The presence of "excess" water in jarosite-type compounds would tend to support such reactions. Based on symmetry considerations, however, Johansson (1963) concluded that three protons (*i.e.*, H_3O^+) were associated with the oxygen occupying the *M* site. Such evidence is not conclusive, of course, nor were the early attempts (Shishkin 1950, 1951) to "prove" the existence of hydronium ion using ionic charge and size effects.

Several efforts have been made to confirm the existence of H_3O^+ in jarosite by infrared spectroscopy. Although such studies have strongly suggested the presence of hydronium ion, they have not proved its existence. Shokarev *et al.* (1972) investigated the spectra of H_3O^+-, K^+-, Na^+- and NH_4^+-jarosites synthesized using water and heavy water, but found no convincing evidence for the existence of H_3O^+. Only a weak band at 1630 cm^{-1} could be assigned to H_3O^+, and this assignment was based solely on the disappearance of the band at 240°C, a tempera-

ture at which H_3O^+ decomposition was expected to occur. Likewise, the spectra of normal and deuterated $H_3OGa_3(SO_4)_2(OH)_6$ determined by Petrov *et al.* (1966) showed a medium-intensity band at 1635–1665 cm^{-1} that might be due to H_3O^+. It was concluded, however, that bands in this spectral region could be assigned equally well to either H_3O^+ or combined H_2O. Kubisz (1972) investigated both normal and deuterated jarosite and alunite over the spectral region 400–3800 cm^{-1}; he concluded that H_3O^+ is present in jarosite, although significant interferences from SO_4^{2-}, H_2O and OH^- were noted. Wilkins *et al.* (1974) concluded that the existence of H_3O^+ in the alunite–jarosite group remained unproved because spectral interferences exist for all the bands that might be assigned to H_3O^+. Most recently, Haley (1984) used low-temperature infrared-absorption spectroscopy to examine synthetic hydronium jarosite and a series of hydronium jarosite – natrojarosite compounds. Although he concluded that hydrated H_3O^+ ions are present, numerous spectral interferences with H_2O, OH^- and SO_4^{2-} were noted, and quantitative agreement between the expected amount of H_3O^+ and the band intensities was not realized. In total, the spectroscopic studies seem to indicate only that hydronium ion might be present; they fail to prove the existence of this species in the alunite–jarosite group.

Under certain conditions, classical broadline ^1H NMR (nuclear magnetic resonance) techniques can distinguish OH^-, H_2O and H_3O^+ groups by utilizing the vastly different proton nuclear dipole–dipole couplings that occur within these groups (Porte *et al.* 1962a, b). Previous work on ^1H lineshapes in alunite is inconclusive with respect to the presence of H_3O^+ (Wilkins *et al.* 1974), although it was shown that some of the protons were in motion at room temperature. A related material, $(H_3O)Ga_3(SO_4)_2(OH)_6$, also was studied by ^1H NMR (Kydon *et al.* 1968, Thompson & Kydon 1974). Rigid-lattice ^1H second moments did not distinguish between $(H_3O^+)Ga_3(SO_4)_2(OH)_6$ and $H_2OGa_3(SO_4)_2(OH)_5 \cdot H_2O$. The observation of a single, low-activation-energy molecular motion was taken as evidence for the presence of H_3O^+ ions, though this evidence is indirect and inconclusive.

Thus, many techniques have been used to try to establish the presence of H_3O^+ in alunite–jarosite compounds, but proof of H_3O^+ is still lacking. Since rotationally mobile D_2O and D_3O^+ groups can have quite distinct ^2H lineshapes (Barnes 1974, O'Reilly *et al.* 1971), this technique was used in the current work to investigate deuterated alunite. Unfortunately, these experiments did not prove the presence of D_3O^+. Protons in such deuterated samples, however, are now "rare" or dilute nuclei (Pines *et al.* 1978), and it is possible to examine the samples with a magic-angle-spinning (MAS) high-resolution ^1H NMR technique (Eckman 1982) to yield a chemical-shift spectrum that is far more diagnostic. Initial studies in the present program were done on jarosite, but the presence of paramagnetic Fe^{3+} is an added complication; the strong magnetic-field-dependent proton–electron dipolar couplings can have profound effects on the NMR spectrum. Consequently, the experiments were done using deuterated alunite, with the certainty that observations made for alunite are equally applicable to jarosite since the two species are isostructural. The present report summarizes work done using both ^1H and ^2H NMR to study the existence of hydronium ion in deuterated hydronium alunite and in hydronium alunite – potassium alunite solid-solution members.

EXPERIMENTAL

Synthesis

The various samples of deuterated hydronium alunite and hydronium alunite – potassium alunite members were synthesized at 170°C in a Parr 2-L autoclave using a glass liner and titanium internals. Dried aluminum sulfate (0.4–1.0 M Al^{3+}) and potassium sulfate (0–0.1 M K_2SO_4) were dissolved in 0.5 L of perdeuterated water. Two and a half grams of $MgClO_4$ were added to ensure passivation of the titanium, and the pH was adjusted to 2.6 or 3.0 with a small amount of H_2SO_4. At the end of the 5-h heating period, the autoclave was rapidly cooled, and the contents were filtered to collect the heavy-water solution. The alunite precipitate was then washed with copious quantities of hot water, and was dried at 110°C.

Alunite characterization

All the products were analyzed chemically for Al, SO_4 and K; total water was determined by difference. X-ray powder patterns were obtained with 114.6-mm Debye–Scherrer cameras using filtered Co$K\alpha_1$ radiation. The back reflections were sufficiently sharp that use of an internal standard to correct for film shrinkage was not necessary. The measured data were least-squares-refined using the procedure and indexing of Jambor & Dutrizac (1983, 1985) and Menchetti & Sabelli (1976). No clearly resolved 11-Å diffraction line was observed on any of the X-ray films, and thus a *c* axis of ≈17 Å was adopted for the refinements. Additionally, all samples were examined using a Guinier–de Wolff focusing camera and Co$K\alpha_1$ radiation to ensure that single-phase compounds had been produced. Previous work has indicated that this technique can detect

TABLE 2. CHEMICAL DATA FOR THE VARIOUS HYDRONIUM ALUNITE - POTASSIUM ALUNITE COMPOUNDS

Sample	%Al	$\%SO_4$	%K	$\%D_2O_{Total}$*	Formula	% Excess Water
Theoretical	20.08	47.66	0.00	32.25	$(D_3O)_{1.00}Al_{3.00}(SO_4)_2(OD)_6$	0.00
H_3O-1	19.60	49.43	0.06	30.91	$K_{0.01}(D_3O)_{0.99}Al_{2.82}(SO_4)_2(OD)_{5.46}(D_2O)_{0.54}$	-1.85
800 A	19.75	48.66	0.02	31.57	$K_{0.00}(D_3O)_{1.00}Al_{2.89}(SO_4)_2(OD)_{5.67}(D_2O)_{0.33}$	-1.03
812	19.16	48.12	2.52	30.20	$K_{0.26}(D_3O)_{0.74}Al_{2.84}(SO_4)_2(OD)_{5.52}(D_2O)_{0.48}$	-0.79
813	17.22	47.88	3.80	31.10	$K_{0.39}(D_3O)_{0.61}Al_{2.56}(SO_4)_2(OD)_{4.68}(D_2O)_{1.32}$	+0.13
814	16.48	46.92	4.82	31.78	$K_{0.50}(D_3O)_{0.50}Al_{2.50}(SO_4)_2(OD)_{4.50}(D_2O)_{1.50}$	+1.37
815	15.44	47.28	5.20	32.08	$K_{0.54}(D_3O)_{0.46}Al_{2.33}(SO_4)_2(OD)_{3.99}(D_2O)_{2.01}$	+1.41
Theoretical	19.26	45.72	9.31	25.71	$K_{1.00}Al_{3.00}(SO_4)_{2.00}(OD)_{6.00}$	0.00

* D_2O totals are by difference from 100%. The % Excess Water is $\%\ D_2O_{Total}$ minus the total water calculated from the formula; i.e., $D_3O^+ + OD^- + D_2O$

~1% of a crystalline impurity in alunite–jarosite compounds. The Guinier films of some of the alunite samples showed a slight separation of the basal diffraction lines; for 003 this separation in 2θ is 0.05° or less (too little to be resolved on the Debye–Scherrer patterns), and the intensities of the split lines are variable from sample to sample. These results indicate that small variations in composition are present, but these are not appreciable relative to the bulk compositions given in Table 2. In other words, some of the products have a slight solid-solution variation, but none is a two-phase mixture of alunite and hydronium alunite. Also, trace amounts of an unidentified impurity phase were detected in sample H_3O–1, but the sample nevertheless was included in the study and did not give anomalous results.

NMR studies

The ^2H NMR lineshapes were recorded at 27.63 MHz on a Bruker CXP–180 NMR spectrometer, and a Bruker–Oxford Instruments cryomagnet. The phase-alternated quadrupole-echo technique (Davis *et al.* 1976) was used with an echo pulse spacing of 35 μs and pulse lengths of 2.6 μs. Temperature variation was achieved by using a gas-flow system and temperature controller; lineshapes at 77 K were recorded by immersing the sample directly in liquid nitrogen.

Dilute ^1H NMR spectra were obtained at 180 MHz at room temperature by making use of the ^1H channel of a probe normally used for ^{13}C cross-polarization and magic-angle-spinning (MAS) studies. A phase-cycled 4-pulse sequence (CYCLOPS) with quadrature detection was used (Redfield & Kunz 1975, Shaw 1984). Magic-angle-spinning rates of 3–3.3 kHz were achieved with Kel–F spinners of the Andrew–Beams type (Andrew 1971). The shifts are given relative to tetramethylsilane (TMS), though in practice a trace of benzene was used in the sample to reference the scale. A background spectrum due to protons in the probe construction was subtracted.

Results and Discussion

Product characterization

Table 2 presents the analytical data obtained for the various samples of deuterated hydronium alunite and hydronium–potassium alunite. All syntheses were done at a pH of 2.6 except for sample H_3O–1, which was prepared at pH 3.0. Attempts to prepare alunite at higher pH values resulted in products contaminated with other basic aluminum sulfates. The two samples of end-member deuterated hydronium alunite (H_3O–1 and 800 A) are close to $D_3OAl_3(SO_4)_2(OD)_6$, although a persistent Al deficiency is characteristic. To maintain charge neutrality in the presence of an Al^{3+} deficiency requires that some of the OD^- be converted to D_2O. This could be accomplished either by a proton in rapid motion among OD^- groups or by a proton statically bound to a given OD^- group. As the measured content of K^+ in an alunite increases, corresponding decreases in the calculated content of D_3O^+ are assumed, such that $K^+ + D_3O^+ = 1.00$. As the K^+ content increases, there is a progressive decrease in Al and a corresponding increase in D_2O to maintain charge neutrality. Significantly, if D_3O^+ is not assumed (*i.e.*, if D_2O were present rather than D_3O^+), then even greater amounts of D_2O must be accommodated to maintain charge neutrality. The amount of "excess water" (*i.e.*, the analytical total less that calculated from the formula) increases steadily as K^+ replaces D_3O^+. There are relatively significant amounts of "excess water" in samples 814 and 815.

TABLE 3. CELL DIMENSIONS FOR ALUNITE - HYDRONIUM ALUNITE SERIES

Sample	K*	Al*	a(Å)	c(Å)	V(Å³)
Kubisz (1970)	0.00	3.00	7.01	17.18	731.1
H_3O-1	0.01	2.82	6.994(6)	17.13(2)	725.6
800 A	0.00	2.89	7.006(4)	17.15(1)	729.0
812	0.26	2.84	6.995(2)	17.14(1)	726.3
813	0.39	2.56	7.004(2)	17.16(1)	729.0
814	0.50	2.50	6.999(3)	17.15(1)	727.5
815	0.54	2.33	7.003(2)	17.16(1)	728.8

*Formula contents K and Al

The results of the X-ray studies (Table 3) show that *a* is about 7.004(2) Å for the hydronium end-member, but that no systematic trend is evident with changing composition, partly because the variation in *a* is minute. Similarly, all values of *c* are identical within the limits of error. These results are surprising when related to K^+-H_3O^+ substitution in jarosite, where *c* increases and *a* and *V* decrease with increasing K^+ (*e.g.*, Brophy & Sheridan 1965). Similar cell-parameter changes were reported by Parker (1962) for K^+-H_3O^+ substitutions in alunite. A notable difference in the present series, however, is that the alunite is nonstoichiometric with respect to Al^{3+}, and that Al^{3+} decreases substantially as the potassium content increases (Table 2). Thus the implication with respect to cell volumes is that decreasing contents of Al^{3+} directly or indirectly negate the expected decrease in volume that attends the substitution of K^+ for D_3O^+. For the formulas in Table 2 it has been assumed that the alkali sites are filled completely by K^+ and $(D_3O)^+$, and thus to rectify the charge imbalance arising from Al^{3+} deficiencies, it also has been assumed that D_2O substitutes for an appropriate amount of OD^-.

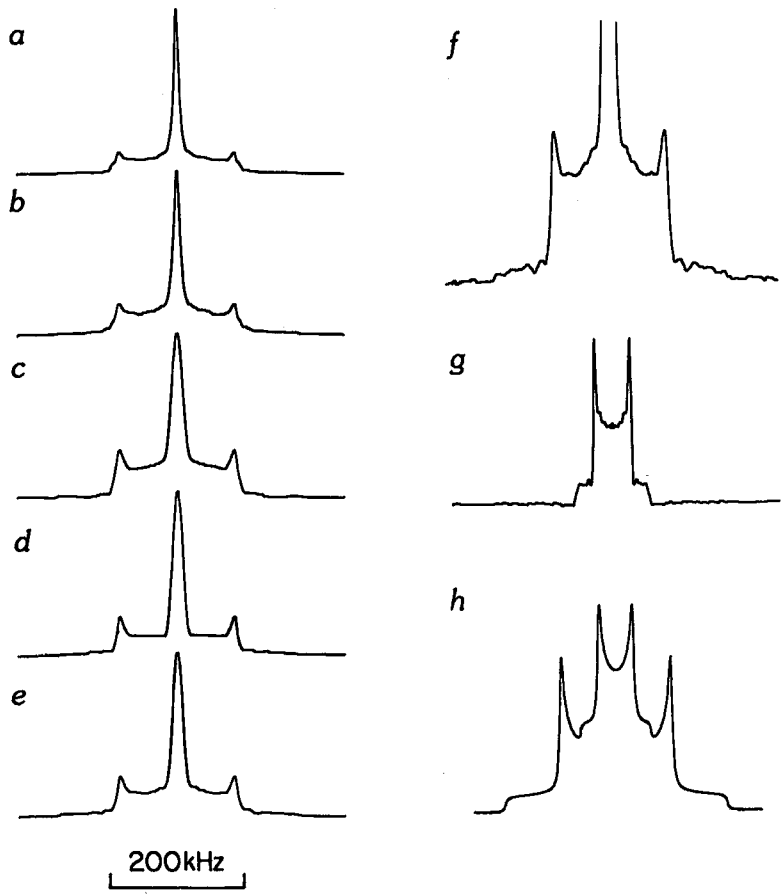

FIG. 1. ^2H NMR lineshapes of alunite at room temperature; a) sample 815, b) 814, c) 813, d) 812, e) 800A, f) 812 × 4, g) ^2H NMR lineshape of D_3OClO_4 at 240 K, C_3 motion, h) calculated ^2H NMR lineshape of $D_3OAl_3(SO_4)_2(OH)_6$ with D_3 motion of D_3O^+ and OD^- rigid.

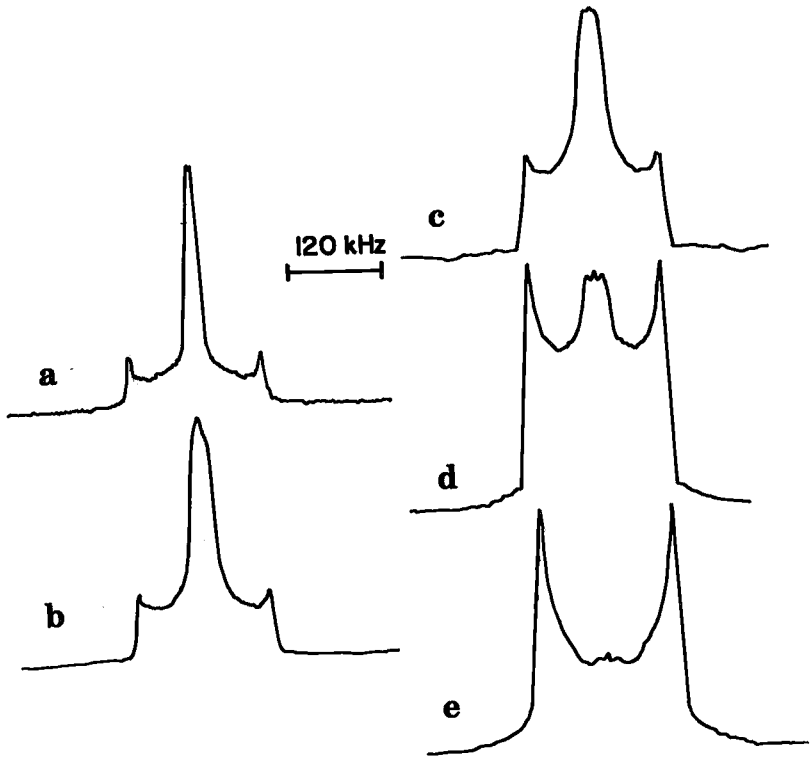

FIG. 2. ^{2}H NMR lineshapes of alunite: H_3O–1 at a) 300 K, b) 160 K, c) 120 K d) 90 K, e) 77 K.

Such D_2O substitutions should expand the cell volume, and in this particular alunite series the effect is to neutralize the contraction that attends K^+ substitution for D_3O^+.

^{2}H NMR lineshapes

The ^{2}H NMR results are shown in Figures 1 and 2. The ^{2}H NMR lineshapes depend on the quadrupole coupling tensor of the ^{2}H nucleus. The tensor is characterized by the quadrupole coupling constant (QCC) equal to e^2gQ/h and the asymmetry parameter ζ (Barnes 1974); in the powder spectrum the tensor gives rise to three pairs of discontinuities (2 if $\zeta = 0$) separated by:

$$\nu_{zz} = 3(QCC)/2$$

$$\nu_{yy} = 3(QCC)(1 + \zeta)/4$$

$$\nu_{xx} = 3(QCC)(1 - \zeta)/4$$

At room temperature all the lineshapes have a broad, outer doublet with a 170-kHz splitting. This splitting corresponds to $\nu_{xx} = \nu_{yy} = 3(QCC)/4$ ($\zeta = 0$), and thus the QCC is 227 kHz. In some instances the outer singularities of the doublet are just visible (Fig. 1f). The doublet can be assigned to the OD^- groups bonded to aluminum, and the magnitude of the QCC indicates that these OD–groups are basically immobile in the structure. Most O–D bonds have characteristic rigid-lattice ^{2}H QCC values of 220 ± 25 kHz (O'Reilly *et al.* 1971, Soda & Chiba 1969) regardless of the molecular group (OD^-, D_2O or D_3O^+), provided that unusually strong hydrogen bonding is not involved. The onset of motion in a group commonly involves reorientation about the group's principal axis of symmetry, and the resulting narrowed ^{2}H lineshape can be much more characteristic of the group than the rigid lineshape. A D_3O^+ group rotating about its C_3 axis has a reduced QCC of approximately 72 kHz with a small asymmetry parameter η (O'Reilly *et al.* 1971), as is shown in Figure 1g for the low-temperature phase of $D_3O^+ClO_4^-$ at 240 K. Figure 1h shows a simulation of the lineshape expected for alunite if all the K^+ ions are replaced by D_3O^+ ions undergoing C_3 rotation, with the OD^- ions still rigid. In contrast, a

D_2O molecule flipping around its C_2 axis in 180° steps typically has a reduced QCC of approximately 120 kHz with $\eta \approx 0.8$–1.0 (Barnes 1974, Soda & Chiba 1969). The component at the centre of the observed room-temperature lineshapes, however, is considerably narrower than the lines for either of these characteristic C_3- or C_2-axis motions. The narrowing indicates more extensive and complex reorientations and, unfortunately, does not permit an assignment to D_3O^+ or D_2O.

It is noticeable that this central component narrows considerably from a half-width of approximately 20 kHz to ~7.5 kHz on going from compositions with high analytical D_3O^+:D_2O values to low values. Taken in conjunction with the ^1H chemical-shift results, it may be inferred that the broader (20 kHz) lineshape is due to reorienting D_3O^+ and the narrower one to D_2O. The width of these narrowed lines indicates that quadrupole couplings are still present, but the absence of distinct doublet-structure then suggests that there is a distribution of motional modes for the group, be it D_3O^+ or D_2O.

When the temperature is reduced, very little change in the lineshape is observed until ~160 K is reached. Below this temperature the narrow line broadens and is reduced in intensity. At approximately 90 K there is some doublet structure visible in the central line, although the fine structure is not sharp. Only a trace of the central line is left at 77 K, and there is a hint of fine structure suggesting that there are now two superimposed broad-doublet components with slightly different quadrupole-coupling constants; one represents the rigid OD^- groups (as in the higher-temperature spectra), and the other represents the D_3O^+ and the D_2O groups, which are now also rigid. The temperature dependence of the spectrum between ~150 K and 77 K is indicative of a gradual freezing-in of molecular motion. The rigid-lattice quadrupole-coupling constant for the group participating in the motion can be estimated to be approximately 246 kHz. The temperature range over which the motion freezes in suggests a low activation-energy for the motion, approximately 12–17 kJ/mol. Furthermore, the motion is not the same for all mobile groups in question, as no distinct quadrupole doublets occur, so that there seems to be no well-defined potential barrier to molecular motion for the group.

In order to understand how this might arise, it is useful to take a close look at the immediate environment of the hydronium ion. Assuming that D_3O^+ replaces K^+ without distorting the local structure, the structural information for alunite derived by X-ray diffraction (Wang *et al.* 1965) may be used to generate the atomic co-ordinates. The origin of the co-ordinate frame can then be moved to a K^+ position. It is then found that the cation is surrounded by 6 sulfate oxygen atoms at 2.82 Å and 6 hydroxyl oxygen atoms at 2.87 Å, which thus fall very nearly on the surface of a sphere. These oxygen atoms take 3-fold positions in 4 planes perpendicular to the 3-fold axis of symmetry (Fig. 3). The positions of the hydrogen atoms of the OD groups are unknown, but they are thought (Wang *et al.* 1965, Menchetti & Sabelli 1976) to interact with the unique O_1 atom of the SO_4^{-2} groups, in which case they would be outside the spherical cavity.

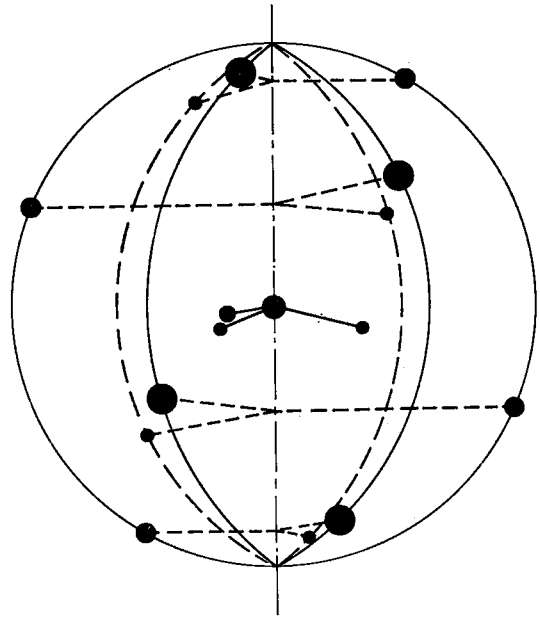

FIG. 3. The twelve oxygen atoms surrounding H_3O^+ on the K^+ site of alunite. Vertical line represents the threefold crystallographic axis.

Assuming that the D_3O^+ oxygen sits at or near the centre of this spherical cavity, then the distances to oxygen atoms on the sphere (2.8–2.9 Å) imply rather weak hydrogen-bonding interaction, if any. Generally, H_3O^+ hydrogen bonds to oxygen in most other well-typified hydronium salts with an average O–H---O hydrogen bond-length of ~2.57 Å (Lundgren & Olovsson 1976). One exception is the room-temperature phase of H_3OClO_4, in which the shortest O–H—O distance is 2.86 Å (Lee & Carpenter 1959), and in which the H_3O^+ ion is known to reorient pseudo-isotropically (O'Reilly *et al.* 1971). Within the sphere of oxygen atoms in alunite, numerous orientations for the H_3O^+ may have very similar potential-energies, with low barriers between them. The inference is, therefore, that the H_3O^+ ion has a high degree of mobility, and this mobility may also explain why X-ray and neutron-diffraction experiments are unsuccessful in locating the H_3O^+ protons. Even at low temperatures, where the ion is effectively rigid, it may well be orientationally dis-

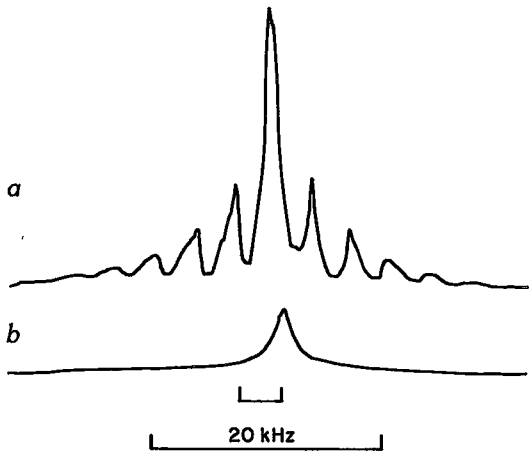

FIG. 4. Dilute ^1H MAS NMR spectrum of a) alunite sample 815 showing spinning sidebands, and b) the probe background. The smaller scale represents the 0–20 ppm chemical-shift scale.

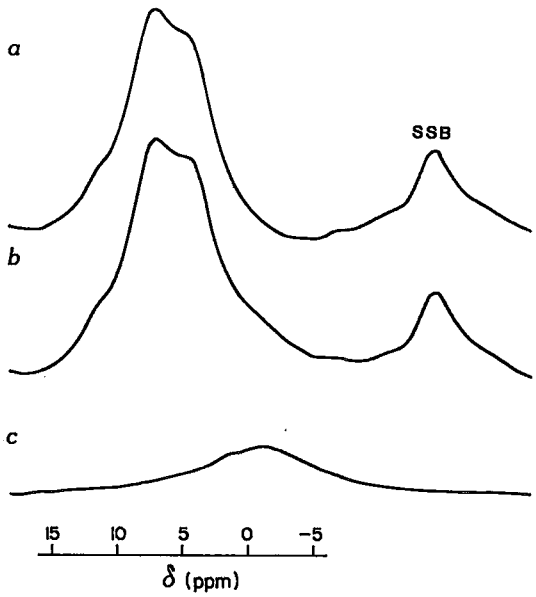

FIG. 5. Dilute ^1H MAS NMR spectrum of alunite sample 815. Spectrum (a) is the corrected spectrum after subtracting background (c) from spectrum (b).

ordered. Similar arguments can be applied equally well to a D_2O molecule substituting for K^+ in the spherical cavity.

One possible model for the motion of D_3O^+ or D_2O within the sphere of oxygen atoms is presented in the Appendix, and is used to calculate a ^2H NMR narrowed line-width. The calculated separation of the inner singularities of the doublet is ~24 kHz, which is reasonably close to the 20 kHz half-width observed for alunite with high D_3O:D_2O values.

Dilute ^1H NMR magic-angle-spinning results

Figures 4 and 5 show the dilute ^1H MAS spectrum of sample 815, and the readily subtracted background spectrum of non-spinning ^1H in the construction materials of the probe. Although only the central component is considered here, considerable intensity is still present in the spinning sidebands (Fig. 4). The spectra of all the samples are shown in Figures 6a–6g. Samples with high analytical D_3O:D_2O values show two main components, at a δ of 11.4 and 4.5 ppm. It is clear that as the ratio decreases, the 11.4 ppm peak also decreases and another band grows at ~7.0 ppm. There is a general relationship (Rosenberger & Grimmer 1979, Freude *et al.* 1982, Berglund & Vaughan 1980) between low-field ^1H shifts and the acidity of the OH proton concerned. This suggests that the three bands at 11.4, ~7.0 and 4.5 ppm are attributable to D_3O^+, D_2O and OD^-, respectively.

Direct and convincing evidence of the band assignments, however, comes from comparison of the shifts noted here with those observed for the same species in other compounds. Because there are few data available for solid-state ^1H NMR shifts (Berglund & Vaughan 1980), an investigation of a range of compounds containing H_2O, OH^-, H_3O^-, $H_5O_2^+$, NH_4^+ and acid groups was carried out, and the results are reported elsewhere (Ratcliffe *et al.* 1985). Figure 6g shows for comparison the spectrum

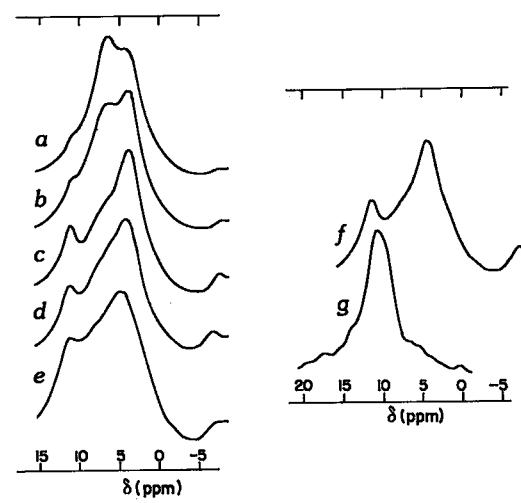

FIG. 6. Dilute ^1H MAS NMR spectra of alunite samples a) 815, b) 814, c) 813, d) 812, e) 800A, f) H_3O–1, g) dilute ^1H NMR spectrum (non-spinning) of D_3OClO_4.

of $H_3O^+ClO_4^-$ in its room-temperature state; this is the classic example of a hydronium compound. The spectrum was obtained without spinning since pseudo-isotropic molecular motion has already averaged out all the dipolar interactions present (O'Reilly *et al.* 1971). The chemical shift of 10.7 ppm agrees very well with the low-field peak in the alunite spectra at 11.4 ppm. The only other reported shift for non-hydrated H_3O^+ is for "magic acid" $HSO_3F/SbF_5/H_2O$ solution in SO_2 (Gold *et al.* 1976); in this solution, the higher resolution shows shifts due to H_3O^+, H_2DO^+ separated by ~0.057 ppm, with a gross shift of 10.3 ppm.

The ~7.0 ppm peak falls into the observed range for H_2O shifts in solids, 7.6–4.2 ppm (Berglund & Vaughan 1980, Ratcliffe *et al.* 1985), and the 4.5 ppm peak falls in the range of assigned OH^- and basic OH in other compounds, 4.6–2.0 ppm (Schreiber & Vaughan 1974, Hunger *et al.* 1983). Obviously the 4.5-ppm peak is in the region of overlap of these two ranges, but since OH^- is present as a major constituent it can be assigned only to this peak.

In an attempt to quantify the amounts of D_3O^+, D_2O and OD^- from the ^1H NMR spectra, a DuPont 310 curve resolver was used to fit the spectra with 3 Lorentzians, the areas of which were then integrated. Some of the fits are very good (Fig. 7), but it must be emphasized that numerous variables and assumptions are hidden in this simplistic fit. Firstly, additional intensity for each species is present in the spinning sidebands and, secondly, the relative intensities in the sidebands may vary depending on the unnarrowed linewidth and lineshape of the individual species. Thirdly, resolution of three closely overlapping peaks may not always have a unique fit, and, fourthly, it is reasonably assumed that the residual protons are distributed evenly among the three chemical species.

The molar ratios of D_3O^+, D_2O and OD^- calculated from the respective ratios of protons determined from the ^1H NMR spectra are compared to the corresponding analytical values in Table 4. The ^1H NMR proton ratio was determined relative to $OD^- = 6.00$, as would be the case for idealized minerals of the alunite–jarosite group. The molar ratios of the various species were then calculated assuming 3, 2 and 1 protons in D_3O^+, D_2O and OD^-, respectively. The agreement between the calculated and analytical data is only fair, although the general trends seem well established. For end-member hydronium alunite (samples H_3O–1 and 800 A), hydronium ion is clearly present, and in amounts close to those predicted from $(D_3O)Al_3(SO_4)_2(OD)_6$. Significant amounts of hydronium ion were also detected in hydronium–potassium alunite (samples 812–815), confirming the hypothesis that H_3O^+ replaces K^+ in alunite–jarosite minerals. Although the ^1H NMR data for

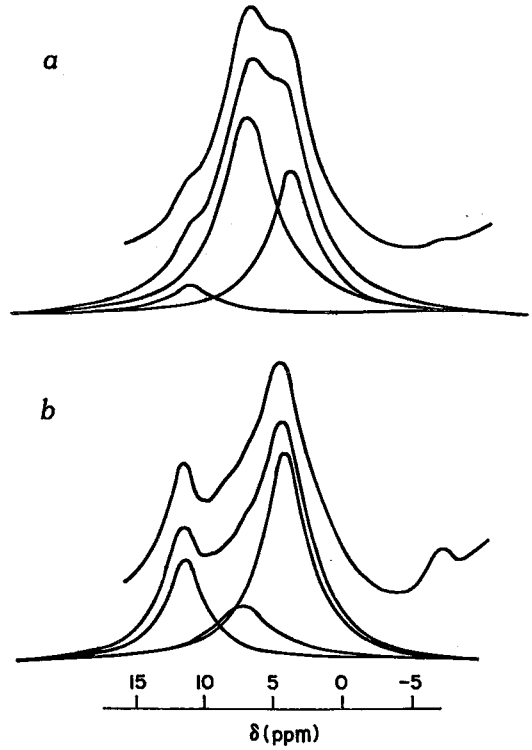

FIG. 7. Three-curve fits (three Lorentzians) of ^1H NMR spectra of alunite (a) 815, (b) H_3O–1, showing the three component curves, their sum and, above each set, the observed spectrum.

D_3O^+ show the expected decline in the D_3O^+/OD^- ratio as the hydronium content of the alunite declines (Table 2), the extent of the decline is somewhat greater than expected. That D_3O^+ was detected in all samples, however, suggests that hydronium ion is not annihilated by associated hydroxyl groups. That is, the reaction

$$H_3O^+ + OH^- \rightarrow 2H_2O$$

does not occur extensively in the alunite–jarosite group, likely because of the strong bonding of OH^- to Al^{3+} or Fe^{3+}.

TABLE 4. ESTIMATED MOLAR RATIOS OF D_3O^+, D_2O AND OD^- FROM THE PROTON-FIT DATA

	^1H NMR Fit			Analytical Ratios			
Sample	D_3O^+	D_2O	OD^-	D_3O^+	D_2O	OD^-	% Excess Water*
H_3O-1	0.83	0.84	6.00	1.09	0.59	6.00	-1.85
800 A	1.13	2.92	6.00	1.06	0.35	6.00	-1.03
812	0.73	2.02	6.00	0.80	0.52	6.00	-0.79
813	0.68	1.34	6.00	0.78	1.69	6.00	+0.13
814	0.51	3.21	6.00	0.67	2.00	6.00	+1.37
815	0.34	4.94	6.00	0.69	3.02	6.00	+1.41

*From Table 2

Significant amounts of water were detected in all the samples, despite the fact that the idealized formula of alunite contains no water. The major cause of the water is likely the *in situ* conversion of OD^- groups to D_2O to maintain charge neutrality resulting from Al^{3+} deficiencies:

$$KAl_3(SO_4)_2(OD)_6 \rightarrow KAl_{3-x}(SO_4)_2(OD)_{6-3x}(D_2O)_{3x} + xAl^{3+}$$

The amount of D_2O calculated by the NMR method, however, is consistently too high. This may have some bearing on the observed ^1H shift of ~7.0 ppm. It is a general trend that for a particular type of molecule, hydrogen bonding causes a downfield ^1H shift. Consequently, the 7-ppm peak may indicate significant hydrogen bonding of the D_2O molecules, presumably to the oxygen atoms of SO_4^{2-} or OD^-. Alternatively, it is conceivable that D_3O^+ hydrogen bonds to the O atoms of excess D_2O; shifts for the peripheral protons of such $H_5O_2^+$ or $H_3O^+ \cdot H_2O$ species have been observed in the 10.1–6.5 ppm range (Ratcliffe *et al.* 1985). Whereas the former is regarded as the more probable explanation of the 7-ppm shift, possibly the latter interaction also contributes, as suggested by Kubisz (1970). A more likely cause of the high calculated contents of water is connected with the problem of the spinning sideband mentioned above. The ^2H NMR lineshapes indicate that the D_2O molecules have the greatest mobility (*i.e.,* the sharpest ^2H spectra). The D_2O, therefore, probably will have the sharpest non-spinning ^1H lineshape. Thus, in the MAS spectra, more of the intensity of D_2O should be concentrated in the central line. Inspection shows that the positions of the peak intensities of the first-order spinning sidebands corresponds to the OD^- line of the centre band. Sideband intensity due to D_2O is much reduced relative to OD^-. Unfortunately, it is not feasible to make comparisons for the much weaker D_3O^+ lines.

Conclusions

Single-phase, deuterated hydronium alunite and hydronium–potassium alunite solid-solution members were synthesized at 170°C from perdeuterated water solutions. The analytical data suggest a continuous variation in the hydronium/potassium ratio, and also indicate persistent deficiencies in Al^{3+}-site occupancy that increase with increasing K^+ content. Dilute ^1H NMR magic-angle-spinning results conclusively demonstrate the existence of hydronium ion in "hydronium alunite" and indicate a charge-compensating substitution of hydronium ion for potassium ion in alunite. The same NMR technique also confirms the presence of large amounts of structural water that originates in part because of deficiencies in Al^{3+}-site occupancy:

$$KAl_{3-x}(SO_4)_2(OH)_{6-3x}(H_2O)_{3x}$$

Additional or "excess water" is still present, however, and may indicate that the hydronium ion itself is partly hydrated. The conclusions concerning hydronium ion and water in alunite most certainly extend to jarosite as well.

References

Andrew, E.R. (1971): The narrowing of NMR spectra of solids by high-speed specimen rotation and the resolution of chemical shift and spin multiplet structures for solids. *Prog. Nucl. Magn. Reson. Spectrosc.* **8**, 1-39.

Barnes, R.G. (1974): Deuteron quadrupole coupling tensors in solids. *Adv. Nucl. Quad. Reson.* **1**, 335-355.

Bengtson, K.B. (1979): A technological comparison of six processes for the production of reduction-grade alumina from non-bauxitic raw materials. *In* Light Metals. The Metall. Soc., Amer. Inst. Mining Metall. and Petroleum Eng., Warrendale, Pennsylvania, 217-282.

Berglund, B. & Vaughan, R.W. (1980): Correlations between proton chemical shift tensors, deuterium quadrupole couplings and the bond distances for hydrogen bonds in solids. *J. Chem. Phys.* **73**, 2037-2043.

Brophy, G.P., Scott, E.S. & Snellgrove, R.A. (1962): Solid solution between alunite and jarosite. *Amer. Mineral.* **47**, 112-126.

_____ & Sheridan, M.F. (1965): Sulfate studies. IV. The jarosite – natrojarosite – hydronium jarosite solid solution series. *Amer. Mineral.* **50**, 1595-1607.

Davis, J.H., Jeffery, K.R., Bloom, M., Valic, M.I. & Higgs, T.P. (1976): Quadrupolar echo deuteron magnetic resonance spectroscopy in ordered hydrocarbon chains. *Chem. Phys. Lett.* **42**, 390-394.

Dutrizac, J.E. (1979): The physical chemistry of iron precipitation in the zinc industry. *In* Lead–Zinc–Tin '80 (J.M. Cigan, T.S. Mackey & T.J. O'Keefe, eds.). The Metall. Soc., Amer. Inst. Mining Metall. and Petroleum Eng., Warrendale, Pennsylvania, 532-564.

_____ (1982): Jarosite-type compounds and their application in the metallurgical industry. *In* Hydrometallurgy Research, Development and Plant Practice (K. Osseo-Asare & J.D. Miller, eds.). The Metall. Soc., Amer. Inst. Mining Metall. and Petroleum Eng., Warrendale, Pennsylvania, 531-551.

_____ (1983): Factors affecting alkali jarosite precipitation. *Metal. Trans.* **14B**, 531-539.

_____ & JAMBOR, J.L. (1985): Formation and characterization of argentojarosite and plumbojarosite and their relevance to metallurgical processing. *In* Applied Mineralogy (W.C. Park, D.M. Hausen & R.D. Hagni, eds.). The Metall. Soc., Amer. Inst. Mining Metall. and Petroleum Eng., Warrendale, Pennsylvania, 507-530.

_____, _____ & CHEN, T.T. (1986): Host minerals for the gallium-germanium ores of the Apex mine, Utah. *Econ Geol.* **81**(4), (in press).

_____ & KAIMAN, S. (1976): Synthesis and properties of jarosite-type compounds. *Can. Mineral.* **14**, 151-158.

ECKMAN, R. (1982): High resolution proton NMR of dilute spins in solids. *J. Chem. Phys.* **76**, 2767-2768.

FREUDE, D., HUNGER, M. & PFEIFER, H. (1982): Study of Bronsted acidity of zeolites using high resolution proton magnetic resonance with magic-angle spinning. *Chem. Phys. Lett.* **91**, 307-310.

GOLD, V., GRANT, J.L. & MORRIS, K.P. (1976): Evidence for the existence of long-lived H_3O^+ (oxonium) ions in solution: NMR spectra of isotopic oxonium ions in HSO_3F–SbF_5 (magic acid) systems. *J. Chem. Soc., Chem. Comm.*, 397-398.

GOREAUD, M. & RAVEAU, B. (1980): Alunite and crandallite: a structure derived from that of pyrochlore. *Amer. Mineral.* **65**, 953-956.

HALEY, L.V. (1984): Determination of hydronium ion in jarosite-type compounds. *CANMET, Energy, Mines and Resources Can., Contract Rep.* **01ST. 23440-2-9076.**

HÄRTIG, C., BRAND, P. & BOHMHAMMEL, K. (1984): Fe-Al Isomorphie und Strukturwasser in kristallen vom Jarosit–alunit-typ. *Z. Anorg. Allg. Chem.* **508**, 159-164.

HUNGER, M., FREUDE, D., PFEIFER, H., BREMER, H., JANK, J. & WENDLANDT, K.-P. (1983): High resolution proton magnetic resonance and catalytic studies concerning Bronsted centers of amorphous Al_2O_3–SiO_2 solids. *Chem. Phys. Lett.* **100**, 29-33.

JAMBOR, J.L. & DUTRIZAC, J.E. (1983): Beaverite–plumbojarosite solid solutions. *Can. Mineral.* **21**, 101-113.

_____ & _____ (1985): The synthesis of beaverite. *Can. Mineral.* **23**, 47-51.

JOHANSSON, G. (1963): On the crystal structure of a basic gallium sulfate related to alunite. *Arkiv Kemi* **20**, 343-352.

KUBISZ, J. (1960): Hydronium jarosite – $(H_3O)Fe_3(SO_4)_2(OH)_6$. *Bull. Acad. Polon. Sci., Ser. Sci. Geol. Geog.* **8(2)**, 95-99.

_____ (1961): Natural hydronium jarosites. *Bull. Acad. Polon. Sci., Ser. Sci. Geol. Geog.* **9(4)**, 195-200.

_____ (1962): Jarositization of rocks in the Upper Silesian coal basin. *Bull. Acad. Polon. Sci., Ser. Sci. Geol. Geog.* **10(1)**, 1-10.

_____ (1964): A study of minerals of the alunite–jarosite group. *Polska Akad. Nauk, Prace Geol.* **22**, 1-93.

_____ (1970): Studies on synthetic alkali–hydronium jarosites. I. Synthesis of jarosite and natrojarosite. *Mineral. Polonica* **1**, 45-57.

_____ (1972): Studies of synthetic alkali–hydronium jarosites. III. Infrared absorption study. *Mineral. Polonica* **3**, 23-37.

KYDON, D.W., PINTAR, M. & PETCH, H.E. (1968): NMR evidence of H_3O^+ ions in gallium sulfate. *J. Chem. Phys.* **48**, 5348-5351.

LEE, F.S. & CARPENTER, G.B. (1959): The crystal structure of perchloric acid monohydrate. *J. Phys. Chem.* **63**, 279-282.

LUNDGREN, J.-O. & OLOVSSON, I. (1976): The hydrated proton in solids. *In* The Hydrogen Bond II (P. Schuster, G. Zundel & C. Sandorfy, eds.). North-Holland, New York, 406-417.

MENCHETTI, S. & SABELLI, C. (1976): Crystal chemistry of the alunite series: crystal structure refinement of alunite and synthetic jarosite. *Neues Jahrb. Mineral. Monatsh.*, 406-417.

O'REILLY, D.E., PETERSON, E.M. & Williams, J.M. (1971): Nuclear magnetic resonance of the aquated proton: hydronium perchlorate. *J. Chem. Phys.* **54**, 96-98.

PARKER, R.L. (1962): Isomorphous substitution in natural and synthetic alunite. *Amer. Mineral.* **47**, 127-136.

PETROV, K.I., PERVYKH, V.G. & BOL'SHAKOVA, N.K. (1966): Infrared absoprtion spectra of basic gallium salts of the alunite type. *Russ. J. Inorg. Chem.* **11**, 742-745.

PINES, A., VEGA, S. & MEHRING, M. (1978): NMR double quantum spin decoupling in solids. *Phys. Rev.* **B18**, 112-125.

PORTE, A.L., GUTOWSKY, H.S. & BOGGS, J.E. (1962a): Proton magnetic resonance studies of polycrystalline uranium oxide hydrates. I. β-$UO_3 \cdot 2H_2O$. *J. Chem. Phys.* **36**, 1695-1699.

_____, _____ & _____ (1962b): Proton magnetic resonance studies of polycrystalline uranium oxide hydrates. II. β-$UO_3 \cdot H_2O$. *J. Chem. Phys.* **36**, 1700-1703.

POSNJAK, E. & MERWIN, H.E. (1922): The system Fe_2O_3-SO_3-H_2O. *J. Amer. Chem. Soc.* **44**, 1965-1994.

RATCLIFFE, C.I., RIPMEESTER, J.A. & TSE, J.S. (1985): NMR chemical shifts of dilute ^1H in inorganic solids. *Chem. Phys. Lett.* **120**, 427-432.

REDFIELD, A.G. & KUNZ, S.D. (1975): Quadrature Fourier NMR detection: simple multiplex for dual detection and discussion. *J. Magn. Reson.* **19**, 250-254.

ROSENBERGER, H. & GRIMMER, A.-R. (1979): Untersuchungen wasserstoff-brückengebundener Substanzen mit Hilfe der hochauflösenden magnetischen Kernresonanzspektroskopie in Festkörpen. I. Zum Zusammenhang zwischen der chemischen Verschiebung der Protonen und dem Charakter der OH-Gruppen in einigen kristallinen Silicaten. *Z. Anorg. Allg. Chem.* **448**, 11-22.

SCHEMPP, C.A. (1923): Argento-jarosite; a new silver mineral. *Amer. J. Sci.* **206**, 73-75.

SCHREIBER, L.B. & VAUGHAN, R.W. (1974): The chemical shift tensor for the hydroxyl proton: $Ca(OH)_2$. *Chem. Phys. Lett.* **28**, 586-587.

SHAW, D. (1984): *Fourier Transform NMR Spectroscopy* (2nd edition). Elsevier, New York, 167.

SHISHKIN, N.V. (1950): Oxonium ions in the structure of inorganic compounds. *Zap Vses. Mineral. Obshchest.* **79**, 94-102 (in Russ.).

_____ (1951): The oxonium ion in the crystal lattices of inorganic compounds. *Zh. Obshchest. Khim.* **21**, 456-467 (in Russ.).

SHOKAREV, M.M., MARGULIS, E.V., VERSHININA, F.I., BEISEKEEVA, L.I. & SAVCHENKO, L.A. (1972): Infrared spectra of iron (III) hydroxide sulphates and hydroxides. *Russ. J. Inorg. Chem.* **17**, 1293-1296.

SODA, G. & CHIBA, T. (1969): Deuteron magnetic resonance study of cupric sulfate pentahydrate. *J. Chem. Phys.* **50**, 439-455.

SZYMAŃSKI, J.T. (1985): The crystal structure of plumbojarosite $Pb[Fe_3(SO_4)_2(OH)_6]_2$. *Can. Mineral.* **23**, 659-668.

THOMPSON, R.T. & KYDON, D.W. (1974): Proton dynamics in hydrated gallium sulfate. *J. Chem. Phys.* **61**, 1813-1815.

WANG, R., BRADLEY, W.F. & STEINFINK, H. (1965): The crystal structure of alunite. *Acta Cryst.* **18**, 249-252.

WILKINS, R.W.T., MATEEN, A. & WEST, G.W. (1974): The spectroscopic study of oxonium ions in minerals. *Amer. Mineral.* **59**, 811-819.

Received November 1, 1985, revised manuscript accepted February 15, 1986.

APPENDIX

^2H line narrowing of D_3O^+ or D_2O in alunite

The degree of ^2H line narrowing can be estimated in a rather simplistic way by assuming that D_3O^+ equilibrium positions are such that each O–D of D_3O^+ is able to reorient with equal probability between positions pointing from the centre of the cavity to each of the 12 surrounding oxygen atoms. These directions make angles of $\pm 68.9°$ or $\pm 31.6°$ with the 3-fold axis of the cavity. If the principal components of the quadrupole-coupling tensor for the rigid O–D are q_{xx}, q_{yy} and q_{zz}, expressions for the motionally averaged (12-position) lineshape can be obtained in a manner basically the same as that described by Barnes (1974) for the simpler case of 2-fold reorientation of a D_2O molecule.

If the Z axis of the co-ordinate system is placed along the 3-fold axis of the cavity, then the orientation of an O–D vector can be described in terms of an angle β between the Z axis and the vector, and a rotation angle α around the Z axis (polar co-ordinates). The tensor can then be written for any orientation as follows:

$$\begin{bmatrix} \cos^2\beta\cos^2\alpha q_{xx} & & \\ & \sin^2\alpha q_{yy} & \\ & & \sin^2\beta\cos^2\alpha q_{zz} \end{bmatrix} \begin{bmatrix} \cos^2\beta\sin\alpha\cos\alpha q_{xx} & & \\ & -\sin\alpha\cos\alpha q_{yy} & \\ & & \sin^2\beta\sin\alpha\cos\alpha q_{zz} \end{bmatrix} \begin{bmatrix} -\sin\beta\cos\beta\cos\alpha q_{xx} & & \\ & 0 & \\ & & \sin\beta\cos\beta\cos\alpha q_{zz} \end{bmatrix}$$

$$\begin{bmatrix} \cos^2\beta\sin\alpha\cos\alpha q_{xx} & & \\ & -\sin\alpha\cos\alpha q_{yy} & \\ & & \sin^2\beta\sin\alpha\cos\alpha q_{zz} \end{bmatrix} \begin{bmatrix} \cos^2\beta\sin^2\alpha q_{xx} & & \\ & \cos^2\alpha q_{yy} & \\ & & \sin^2\beta\sin^2\alpha q_{zz} \end{bmatrix} \begin{bmatrix} -\sin\beta\cos\beta\sin\alpha q_{xx} & & \\ & 0 & \\ & & \sin\beta\cos\beta\sin\alpha q_{zz} \end{bmatrix}$$

$$\begin{bmatrix} -\sin\beta\cos\beta\cos\alpha q_{xx} & & \\ & 0 & \\ & & \sin\beta\cos\beta\cos\alpha q_{zz} \end{bmatrix} \begin{bmatrix} -\sin\beta\cos\beta\sin\alpha q_{xx} & & \\ & 0 & \\ & & \sin\beta\cos\beta\sin\alpha q_{zz} \end{bmatrix} \begin{bmatrix} \sin^2\beta q_{xx} & & \\ & 0 & \\ & & \cos^2\beta q_{zz} \end{bmatrix}$$

To find the motionally averaged tensor, the components must then be averaged over the 12 orientations:

β	α
+68.9	0, ±120
-68.9	±60,180
+31.6(17)	±60,180
-31.6(17)	0, ±120

Non-diagonal terms reduce to zero, and the end results is:

$$q'_{xx} = q'_{yy} = \tfrac{1}{4}[q_{xx}(0.8547716) + 2q_{yy} + q_{zz}(1.145228)]$$

$$q'_{zz} = \tfrac{1}{2}[q_{xx}(1.145228) + q_{zz}(0.8547716)]$$

The q' values are the narrowed tensor components, and it should be noted that the lineshape is axially symmetrical. If the rigid tensor were also axially symmetrical (*i.e.*, $q_{xx} = q_{yy}$), then the motionally narrowed lineshape calculated as above would be only 0.1411 as wide. That is, if the inner singularities of the rigid lineshape (q_{xx}) are separated by 170–180 kHz, then in the narrowed lineshape (q'_{xx}) they will be separated by 24–25.4 kHz.

It must be emphasized that this is only *one* crude model and that it does not account for the absence of singularities in the observed lineshapes, but the width calculated is of the same order.